DYNAMIC PROPERTIES OF SHERMAN ISLAND PEAT

By Ross W. Boulanger,[1] Rajendram Arulnathan,[2] Leslie F. Harder Jr.,[3] Ralphael A. Torres,[4] and Michael W. Driller[5]

ABSTRACT: The dynamic properties of peat have been identified as major source of uncertainty in the evaluation of seismic hazards throughout the Sacramento–San Joaquin Delta in northern California. This paper summarizes the results of a laboratory study of the dynamic properties of a layer of peaty organic soil underlying the south levee on Sherman Island near the western side of the delta. Conventional Shelby tube sampling procedures were able to obtain high-quality samples because of the compactness of this peat layer, located between depths of 9 and 16 m. The samples tested were very fibrous and had ash contents of 35–56%. Staged cyclic triaxial loading was used to measure the stress-strain behavior of several specimens under cyclic shear strains ranging from about 0.0005% to 10%. Other tests included piezo-ceramic bender element tests to measure the shear wave velocity of specimens within the triaxial device, and undrained monotonic triaxial compression and extension tests. The effects of loading frequency, cyclic degradation, consolidation stress history, and structural anisotropy are evaluated. The resulting modulus reduction and damping relationships for the Sherman Island peat are compared with published results for other peats, solid waste materials, and mineral soils.

INTRODUCTION

The Sacramento–San Joaquin Delta in northern California contains over 60 low-lying "islands" with ground levels below sea level. These islands are protected against inundation from adjoining rivers and sloughs by over 1,700 km of levees. These levees have been generally constructed of uncompacted sands, silts, clays, and peat; thick deposits of peat and highly organic soils underlie the levees across much of the delta. The expected seismic response of these levees, which affects the potential for liquefaction of the cohesionless materials within the levees, depends on factors that include the subsurface stratigraphy (layering sequence and layer thickness), dynamic properties of each stratum, frequency content of the earthquake, level of shaking, and duration of shaking. Reasonable guidance regarding most of these factors can be found in the technical literature. There are, however, only limited experimental data regarding the dynamic properties of peat and highly organic soils. Consequently, an improved understanding of the dynamic properties of organic soils has been identified as a primary need in future evaluation of seismic hazards throughout the Sacramento–San Joaquin Delta (*Seismic* 1992).

Previous research on the dynamic properties of peat include efforts by Seed and Idriss (1970), Kramer (1993, 1996), and Stokoe et al. (1994). Note that the term "peat" will hereafter be used to refer to both peat and peaty organic soils. Seed and Idriss (1970) analyzed the motions recorded at an 18 m deep deposit of unconsolidated peat at Union Bay during a magnitude 4.5 earthquake. "Unconsolidated" is used to describe peat that has been consolidated only by its own largely submerged weight. For example, 18 m of submerged peat with a total unit weight of 10.2 kN/m^3 will generate an effective overburden pressure of only 7 kPa. Seed and Idriss concluded that peat exhibited stronger nonlinearity and higher damping ratios than clays (shown later in Fig. 12). Although their modulus reduction and damping curves for peat have been widely used, Idriss (personal communication) has conveyed to his colleagues that these studies needed to be revisited and the resulting curves likely revised.

Stokoe et al. (1994) presented results for two peat specimens from a bridge site in New York tested in a resonant column and torsional shear device. These two specimens had water contents of 210 and 285% and ash contents of 37 and 65%; they came from depths of about 9 m, where the in situ vertical effective stress was about 114 kPa. Each specimen was subjected to a series of resonant column and torsional loadings at six different consolidation stresses, various durations of confinement, and various loading frequencies. The test results showed very linear behavior, with negligible modulus reduction (i.e., $G/G_{max} > 0.98$) and low damping ratios (<3% for <1 Hz loading) at shear strains ranging up to 0.1%. Shear moduli increased by 5–8% per log cycle increase in loading frequency (using 1 Hz as the reference frequency), based on tests with cyclic shear strains of 0.001%, 0.01%, and 0.1% and loading frequencies of 0.1–30 Hz. Damping ratios also increased with loading frequency, with variable differences of 0.0–0.9% damping per log cycle of loading frequency.

Kramer (1996) presented results of resonant column tests in a follow-up to an earlier study involving cyclic triaxial and piezo-ceramic bender element tests (Kramer 1993). Both studies used tube samples of peat from Mercer Slough in Washington, which is a fibrous peat with an in situ water content of 500–1,200%. Specimens were consolidated to effective confining pressures of 1.5–12 kPa for the resonant column tests and about 19 kPa for the cyclic triaxial tests. Kramer (1996) concluded that the variation of modulus reduction (G/G_{max}) and damping with shear strain for Mercer Slough peat depended on the effective confining pressure, with the peat showing more linearity (i.e., higher G/G_{max} ratios and lower damping) with increasing effective confining pressure.

This paper presents the results of a laboratory study of the dynamic properties of a layer of consolidated peat underlying the south levee of Sherman Island near the western side of the Sacramento–San Joaquin Delta in northern California. Subsurface conditions, sampling and laboratory testing procedures, and experimental results are presented in detail because only limited data are currently available for peat. The effects of loading frequency, cyclic degradation, consolidation stress history, and structural anisotropy are evaluated. The resulting modulus reduction and damping relationships for the Sherman

[1]Asst. Prof., Dept. of Civ. and Envir. Engrg., Univ. of California, Davis, CA 95616.
[2]Grad. Student, Dept. of Civ. and Envir. Engrg., Univ. of California, Davis, CA.
[3]Chf. of Engrg., Dept. of Water Resour., State of California, Sacramento, CA 94236.
[4]Chf. of Canals & Levees Sect., Dept. of Water Resour., State of California, Sacramento, CA.
[5]Sr. Engr., Dept. of Water Resour., State of California, Sacramento, CA.

Note. Discussion open until June 1, 1998. To extend the closing date one month, a written request must be filed with the ASCE Manager of Journals. The manuscript for this paper was submitted for review and possible publication on April 29, 1997. This paper is part of the ***Journal of Geotechnical and Geoenvironmental Engineering***, Vol. 124, No. 1, January, 1998. ©ASCE, ISSN 1090-0241/98/0001-0012–0020/$4.00 + $.50 per page. Paper No. 15719.

Island peat are compared with published results for peats, mineral soils, and solid waste materials.

SAMPLING LOCATION AND PROCEDURES

South Levee on Sherman Island

Samples of peat were obtained from borings along the south levee on Sherman Island near the western side of the delta. These borings were located next to a down-hole array of accelerometers installed through the levee crest by the Department of Water Resources, State of California (CDWR), in 1995. A schematic cross section of the subsurface conditions at the sampling location is shown in Fig. 1.

Results from a CPT sounding and a boring with down-hole shear wave velocity (V_s) measurements using the OYO Suspension P-S logging system are shown in Fig. 2. These explorations were approximately 5–10 m from the sampling locations. Note that CPT-derived B_q parameter in Fig. 2 is given by $B_q = (u_{bt} - u_o)/(q_c - \sigma_v)$, where u_{bt} = pore pressure measured behind the cone tip; u_o = hydrostatic pore pressure; q_c = tip resistance (corrected for area effects); and σ_v = total vertical stress. While Figs. 1 and 2 focus on the upper 25 m of stratigraphy, it should be noted that the soil deposits in this area are hundreds of meters thick and that their characteristics are also important in assessing the seismic response of the levees.

The levee materials generally consist of peat and dredged sand, silt and clay, with compacted sandy fill along the crown (Figs. 1 and 2). Beneath the levee is a thick layer of peat with sandy micaceous silt interlayers. This peat layer is typically about 12 m thick in the fields away from the levee but has been highly compressed under the weight of the levee. Underlying the peat is an approximately 8 m thick layer of silty clay, under which is a sand stratum.

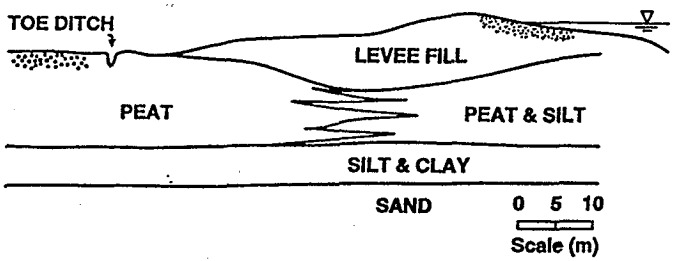

FIG. 1. Schematic of Typical Sherman Island Levee

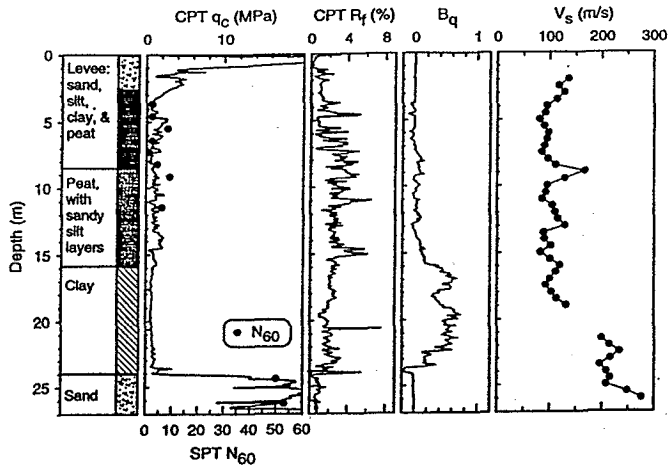

FIG. 2. CPT and Shear Wave Velocity Data at Sherman Island

General Characteristics of Peat Layer

The peat layer between depths of 9 and 16 m beneath the levee (Figs. 1 and 2) was the subject of this study. Characteristics of the samples used for triaxial testing, all from depths of 12–14 m in this layer, are summarized in Table 1. The peat at these depths has a highly fibrous fabric from which individual fibers 1–3 cm long can readily be unraveled. The primarily horizontal orientation of the fibers is visually apparent and is demonstrated by a relatively easy separation of samples along horizontal planes (a sharp knife is needed to split samples along vertical planes). Samples tested in this study had water contents of 152–240% and ash contents of 35–56%.

The peat samples tested in this study may alternatively be described as highly organic soils, since the ash content is greater than 25%, based on ASTM D4427 "Classification of Peat Samples by Laboratory Testing." Nonetheless, in this paper, the samples from Sherman Island will be referred to as peat because of their highly fibrous nature and because "peat" is the term many geotechnical engineers would use to describe these types of highly organic soil deposits based on ASTM 2487 "Classification of Soils for Engineering Purposes."

Consolidation tests on peat samples (Roger Foott Associates 1991) from a nearby section of levee indicate that the peat layer is nearly normally consolidated beneath the adjacent fields landward of the levee but is overconsolidated beneath the levee. Preconsolidation pressures beneath the levee were

TABLE 1. Summary of Triaxial Testing Program and Sample Characteristics

Test number (1)	Sample number (2)	Depth (m) (3)	Water content (%)[a] (4)	Ash content (%)[b] (5)	Total γ (kN/m^3) (6)	In situ σ'_{vo} (kPa) (7)	Triaxial σ'_{3c} (kPa) (8)	Bender V_s (m/s) (9)	Type of triaxial test (10)
1	5D-P4(1)	13.6	200	56	11.5	136	200	81.5	Cyclic
2	5E-S2(1)	13.5	180	54	11.3	132	132	—[d]	Cyclic
3	5E-S2(2)	13.4	202	41	11.2	132	132	80.9	Cyclic
4	5E-S2(3)	13.2	185	42	11.3	131	131	86.4	Cyclic
5	5G-S4(1)	13.7	196	54	11.3	136	136	84.0	Cyclic
6	5G-S4(2)	13.5	186	37	11.3	132	132	83.2	Cyclic
7	5G-S4(3)	13.3	240	42	11.1	131	200	87.9	Cyclic
8	5F-S4(1)	13.7	164	37	11.4	136	136	—[e]	Compression
9	5F-S4(2)	13.5	169	37	11.6	132	66[c]	86.6	Cyclic
10	5F-S4(3)	13.3	194	35	11.4	132	66[c]	82.6	Cyclic
11	5G-S3(1)	12.9	152	36	11.8	130	130	—[e]	Extension
12	5G-S3(2)	12.8	205	44	11.2	128	128	87.0	Cyclic

[a]Oven drying temperature of 90°C.
[b]ASTM D2794 standard (1991).
[c]Specimen was first consolidated to a σ'_{3c} of 132 kPa and then rebounded to a σ'_{3c} of 66 kPa.
[d]Bender element did not function.
[e]Bender elements were not installed in the triaxial device that was used for monotonic loading tests.

about 120–220 kPa; the estimated effective overburden stresses were 95–115 kPa over the corresponding depths. Overconsolidation of the peat beneath the levee may be caused by desiccation during the progressive buildup of natural levee deposits along the river channel, or by long-term secondary compression under the weight of the levee.

Shelby Tube Sampling and Handling

Shelby tube samples of the peat between depths of 12 and 14 m were obtained in hollow stem auger borings. A high water level was maintained in the hollow auger to ensure outward seepage at the bottom of the boring. Sample quality appeared very high, with 100% recovery in most cases. The high sample quality was attributed to the relatively compact nature of the peat beneath the levee and contrasted sharply with the difficulty of sampling unconsolidated peat in the fields away from the levees. Samples were immediately sealed, placed upright in a padded box, and transported to the laboratory, where they were stored in a chamber at 13°C and greater than 96% humidity. X-ray photographs of the sample tubes were taken to aid in selecting intervals for testing. The first specimen was tested about one week after drilling, and subsequent tests averaged about one week each to complete.

TRIAXIAL TESTING EQUIPMENT AND PROCEDURES

Cyclic Triaxial Equipment

All tests were performed in a cyclic triaxial device designed to measure stress-strain behavior over a wide range of strains (Gookin et al. 1996). Axial strains are measured three ways to provide overlapping data: High-resolution proximity transducers and a LVDT located on the top platen inside the cell measure small strains, and another LVDT located outside the cell measures large strains. Loads for very small strains are measured using a low-capacity, protected load cell inside the cell, while loads at larger strains are measured using a larger-capacity load cell outside the cell. In addition, cantilever-type, piezo-ceramic bender elements are mounted in the top and bottom platens to measure shear wave velocities (V_s) before cyclic loading and thereby obtain the maximum shear modulus (G_{max}).

Effect of End Conditions on Strain Measurements

Tatsuoka et al. (1994) reported that axial strains measured from the top platen in triaxial tests on granular soils tend to be larger than those measured locally on the specimen; they attribute the difference to bedding errors between the specimen and the end platens. Tatsuoka et al. (1994) concluded that bedding errors were important except in tests on soft clays. Since the Sherman Island peat specimens are as soft as most soft clays, their conclusion suggests that axial strain measurements from the end platens would be as accurate as local strain measurements in the current study.

Experience with small-strain measurements on sand specimens has shown good agreement between local and end platen measurements, with the local strain measurements being slightly greater in some cases (Gookin et al. 1996). The good agreement between local strain measurements and end platen measurements is attributed to the nonlubricated end conditions, the porous stones being small inserts in the end platens, and the use of internal proximeter transducers with much greater resolution than those used by Tatsuoka et al. (1994). (The full range of the proximeter transducers used in this study cover an axial strain of only 0.02%, whereas Tatsuoka et al. used proximeter transducers that covered axial strains as great as 5%.) Consequently, local strain measurements were not considered necessary in the current study because of previous experience with high-resolution proximeter transducers and the soft nature of the peat being tested.

Sample Preparation and Consolidation

Specimens 15–17 cm tall and 7.1 cm in diameter were extruded and the ends trimmed using the procedures described by Boulanger et al. (1997). A membrane was then placed around the specimen, a full vacuum applied for typically one hour, and the specimen transferred to the triaxial cell for testing.

Specimens were first back-pressure saturated with a back-pressure of typically 100 kPa, while the effective confining stress was maintained constant at about 100 kPa. Specimens were then isotropically consolidated to the desired confining stress. End-of-primary consolidation typically took about 12 hours, after which about six hours of secondary compression was allowed to occur. Drainage lines were then closed, and the specimen left for typically one hour to allow pore pressures to stabilize. The pore pressure rise due to undrained creep during this last hour was typically 4–10% of the isotropic effective consolidation stress.

The testing sequence began with a bender element test, which was followed by a series of staged cyclic loading tests as described in a following section. B-values were measured before cyclic loading and just after cyclic testing; all but one specimen had B values greater than 0.96 at both times. The specimen in test no. 10 had a B value of only 0.82, but, interestingly, its behavior during cyclic loading was indistinguishable from that of the other specimens.

BENDER ELEMENT TESTS

Interpretation of Bender Element Signals

Bender element tests were performed before cyclic loading, and the measured shear wave velocity (V_s) was used to calculate G_{max} as

$$G_{max} = \rho \times V_s^2 \tag{1}$$

where ρ = density of the specimen. Time histories of the transmitted signal and the received signal for a typical test are shown in Fig. 3(a). There are several methods of interpreting the travel time (and therefore V_s) of the shear waves in the soil, based on the transmitted and received signals. One approach is the use of characteristic points (usually the peaks): Travel time is taken as the time between point A on the transmitted signal and point A′ on the received signal (or B to B′). A second approach is the use of cross-correlation techniques: The transmitted and received signals are cross-correlated as

$$CC(\tau) = \int_{-\infty}^{\infty} S_1(t + \tau) \times S_2(t)\, dt \tag{2}$$

where S_1 = transmitted signal; S_2 = received signal; τ = time shift applied to S_1; and $CC(\tau)$ = cross-correlation. Travel time is then the time shift, τ, producing the peak cross-correlation [point D in Fig. 3(b)]. However, the use of either of these methods is appropriate only when the same plane wave is measured at two spaced points. This necessary condition is not satisfied in the triaxial device for three main reasons (Arulnathan et al. 1997): (1) the signals are affected by waves reflected from the relatively rigid end platens, and therefore represent a complex interaction of incident and reflected waves; (2) there are phase (or time) lags between the electrical signals and the physical waves in the soil, particularly at the transmitting bender element; and (3) non-one-dimensional wave travel and near-field effects are not accounted for. These errors can cause an overestimation or underestimation of V_s depending on the test conditions (Arulnathan et al. 1998).

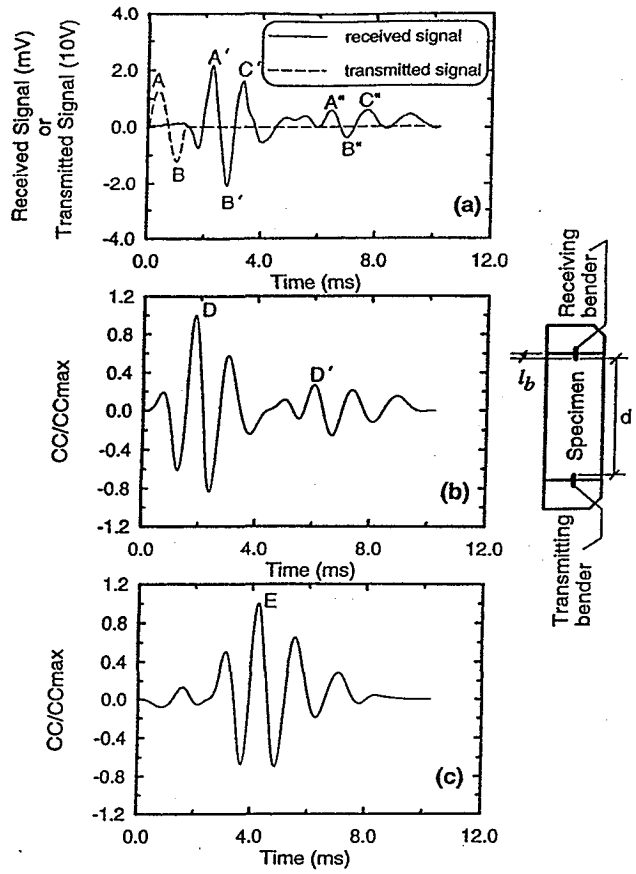

FIG. 3. Bender Element Results for Test No. 1: (a) Transmitted and Received Signals; (b) Cross-Correlation of Transmitted and Received Signals; (c) Cross-Correlation of First and Second Arrivals in Received Signal

An alternative approach to interpretation of bender element tests is to use the second arrival in the received signal: The second arrival refers to the part of the signal that is produced when the originally transmitted wave arrives at the receiver cap for the second time. Travel time is estimated using the time between the characteristic peaks A′ and A″ (or B′ and B″, C′ and C″) in Fig. 3(a) (Arulnathan et al. 1997). Similarly, the received signal can be cross-correlated with itself to obtain the travel time between the first and second arrivals. For clarity, this is done by breaking the received signal into two dummy signals prior to cross-correlating them: One dummy signal contains the first arrival and zero signal elsewhere, and the other dummy signal contains the second arrival and zero signal elsewhere. This approach was used to produce the cross-correlation in Fig. 3(c), in which the travel time is at point E. Note that this approach can yield an answer that is very nearly the same as the difference between points D and D′ in the cross-correlation of the input and output signals [Fig. 3(b)]. The first and second arrivals of the shear wave at the receiver cap are equally affected by two sources of error—wave reflection, and phase lags between electrical and physical wave. The errors due to non-one-dimensional wave travel and near-field effects, however, are expected to cause the second arrival methods to slightly underestimate V_s.

Table 2 compares V_s values calculated through the previously described procedures for the test shown in Fig. 3. The methods that use the transmitted and received signal gave V_s values of 87–89 m/s for this specimen, while the second arrival methods gave V_s values of about 81–82 m/s. Therefore, the methods that use the transmitted and received signals gave V_s values that were about 8% greater than the V_s values obtained through second arrival methods, which corresponds to a 17% difference in G_{max} values.

TABLE 2. Comparison of V_s Interpretation Methods for Test No. 1

Interpretation method (1)	Using transmitted and received signals (2)	Using first and second arrivals in received signal (3)
Characteristic peaks	87.3 m/s[a]	81.3 m/s[b]
Cross-correlation	88.7 m/s	81.7 m/s[c]

Note: Input signal frequency was 1.1 kHz. The resulting ratio of wavelength (λ) to bender element length (l_b) was $\lambda/l_b = 15$, and the ratio of wave travel distance for first arrival ("d" in Fig. 3) to λ was $R_d = d/\lambda = 2.3$.

[a]Using the average of the travel times indicated by the two strongest peaks in the signals.

[b]Using the average of the travel times indicated by the three strongest peaks in the signals.

[c]Received signal split into two dummy signals containing first and second arrivals, respectively.

Comparison of In Situ and Laboratory Shear Wave Velocities

The results of the bender element tests, based on the second-arrival methods and summarized in Table 1, showed V_s values ranging from 81 to 87 m/s (with an average of 84 m/s) for the specimens that were reconsolidated to their in situ vertical effective stress. These samples were obtained between depths of 12.8 and 13.7 m, and were specifically selected for their high organic contents. The corresponding OYO V_s measurements at these depths (Fig. 2) show V_s values ranging from approximately 83 to 90 m/s. Slightly higher V_s values were recorded at other depths within the peat layer (9.5–15.5 m depth), but a comparison of the borehole logs and the V_s profile indicates that these higher V_s values tend to occur where there are sandy silt interlayers. Thus, the in situ and laboratory V_s data agree, which suggests that the low strain shear moduli of the laboratory specimens were not significantly affected by sampling disturbance.

CYCLIC TRIAXIAL TESTING

A summary of the cyclic testing program is given in Table 1. Six specimens were isotropically consolidated to an effective stress (σ'_{3c}) equal to their in situ vertical effective stress (σ'_{vo}) of about 132 kPa. Two specimens were consolidated to about 200 kPa, or about 1.5 times their σ'_{vo}. Another two specimens were consolidated to their σ'_{vo} of about 132 kPa, and then rebounded to a σ'_{3c} of 66 kPa to evaluate the effects of stress history. Measurements of axial strain (ε_a) and axial Young's modulus (E_a) from undrained loading of these saturated specimens were converted to equivalent shear strain (γ) and shear modulus (G) as $\gamma = 1.5\varepsilon_a$ and $G = E_a/3$.

Undrained, strain-controlled cyclic testing was performed in stages on each specimen as follows. Each stage consisted of five uniform cycles at a strain level greater than was used in the previous stage. For shear strains (single amplitude) less than about 0.001%, some stages were repeated a second time to obtain less noisy measurements, or the strain level was increased by a factor of 1.5–2.0 for the next stage of cycles. For shear strains above 0.001%, the strain levels for each stage were generally increased by about one-half of a log-cycle (i.e., by a factor of about 3). Specimens remained undrained throughout all stages of loading. In these staged testing procedures, the effect of prior stages of cyclic loading on the secant shear modulus, measured in the fifth cycle of a subsequent stage of loading, was expected to be small (Tatsuoka et

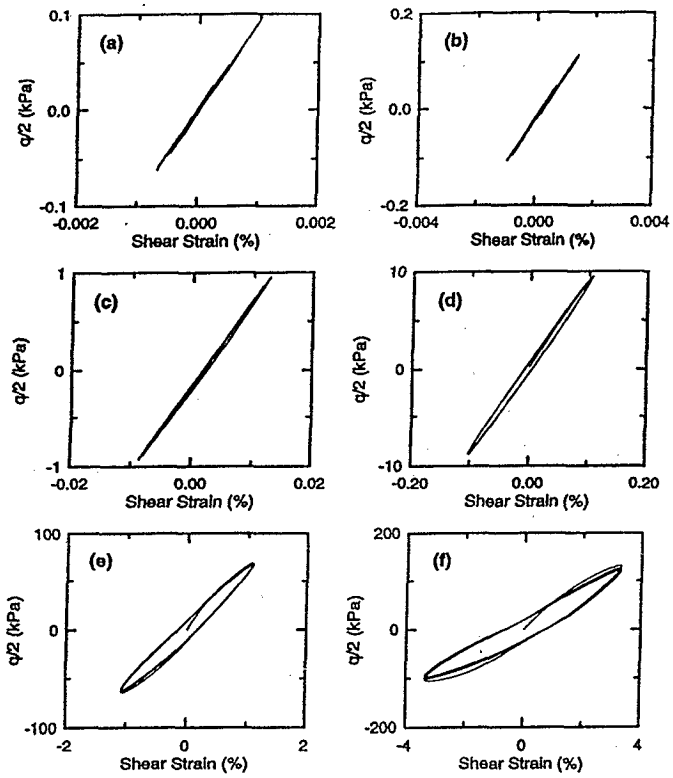

FIG. 4. Stress-Strain Curves for Test No. 1

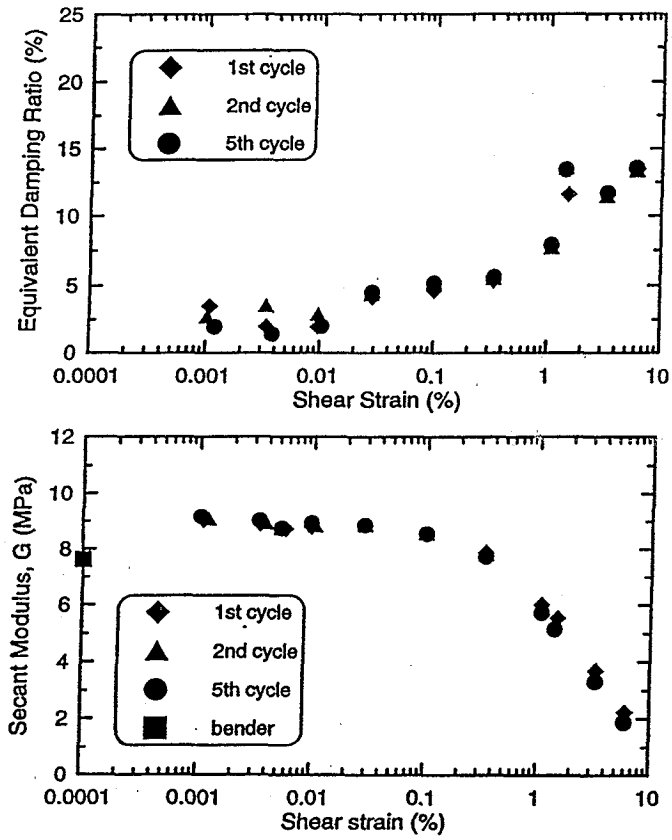

FIG. 5. Secant Modulus and Equivalent Damping Ratio versus Shear Strain for Test No. 1

al. 1991). The reasonableness of taking this approach to these peats was later verified by the test data (in the following section), which showed that the rate of cyclic degradation was relatively small.

The loading frequency for all cyclic tests except no. 12 (see Table 2) was 1.0 Hz for cyclic shear strains of up to 5%, after which it was reduced to 0.25 Hz due to the limitations of the hydraulic loading system. For test no. 12, loading frequencies of 0.01 Hz and 1.0 Hz were used for different stages to evaluate frequency effects.

Typical cyclic test results are shown by the stress-strain curves for test no. 1 in Fig. 4, and the corresponding plots of secant modulus and equivalent damping ratio versus shear strain (single amplitude) in Fig. 5. The stress-strain curves in Fig. 4 show almost linear behavior for shear strains of up to 0.1%, and very little degradation with increasing number of loading cycles even for shear strains of 3%. Noise in the stress and strain measurements at shear strains less than about 0.001% was reduced using a 6–10 Hz low-pass filter. These filtering procedures had essentially no effect on the calculation of secant shear modulus but did improve the reliability of equivalent damping ratio calculations.

The effects of loading frequency and cyclic degradation on shear modulus are illustrated in Fig. 6, which shows the variation in secant shear modulus with number of loading cycles for test no. 12. Thirty cycles of loading were applied at shear strains of 0.003% [Fig. 6(a)], 0.01% [Fig. 6(b)], and 1.0% [Fig. 6(c)]. At each stage, the 30 cycles of loading were applied as alternating sets of five cycles at 1.0 Hz and 0.01 Hz.

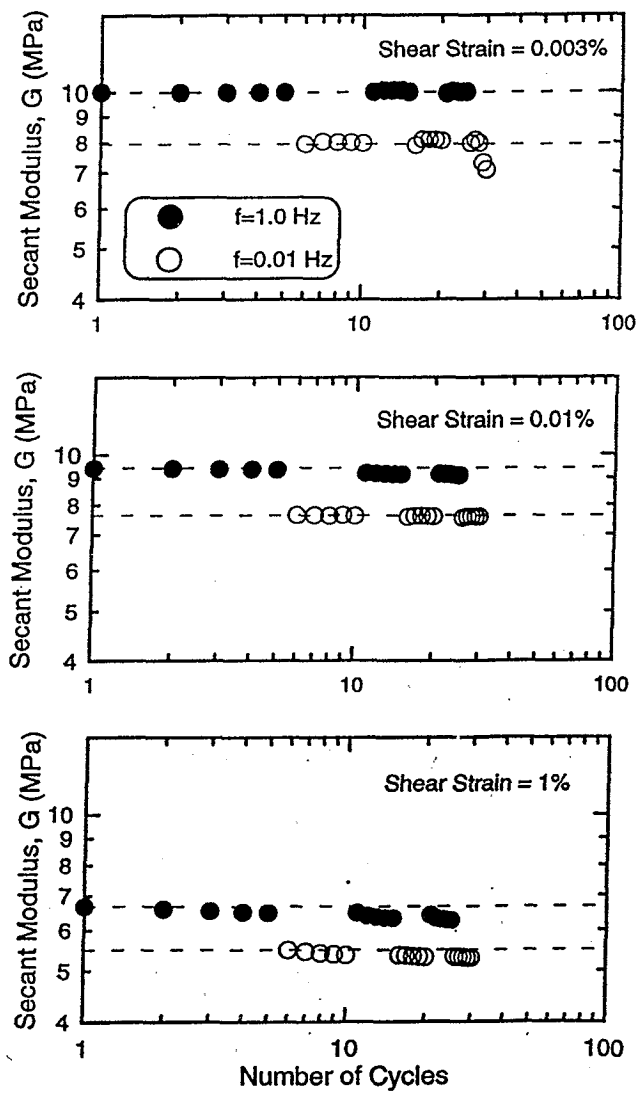

FIG. 6. Effect of Loading Frequency and Cyclic Degradation on Secant Modulus for Test No. 12

The effect of loading frequency was similar at all three shear strain levels, with the secant modulus being about 15–20% lower at the lower loading frequency. This difference corresponds to about an 8–10% change in secant modulus per log cycle of loading frequency (using 1 Hz as the reference frequency).

The data in Fig. 6 also show that cyclic degradation of the secant modulus was very minor even at cyclic shear strains of 1%. The effect of cyclic degradation can be expressed by the degradation index (δ), which is the ratio of the secant modulus in cycle N (G_N) to the secant modulus in the first cycle (G_1). The value of δ decreases with increasing cycles and can be approximately represented, according to Idriss et al. (1978), as

$$\delta = N^{-t}$$

where t = degradation parameter. For the data in Fig. 6, the value of t was only about 0.017 at cyclic shear strains of 1%. [For comparison: Vucetic and Dobry (1991) used $t = 0.06$ to represent high-plasticity ($PI \approx 50$) clays.]

The variation of equivalent damping ratio during the same test as shown in Fig. 6 (test no. 12) is shown in Fig. 7. Equivalent damping ratios are smaller at the higher loading frequency (1.0 Hz) than at the lower loading frequency (0.01 Hz). The difference between the equivalent damping ratios at 1 Hz and 0.01 Hz increased as the cyclic shear strain was increased. The observed decrease in damping ratio with increasing loading frequency for this specimen is opposite to the effect on peat reported by Stokoe et al. (1994).

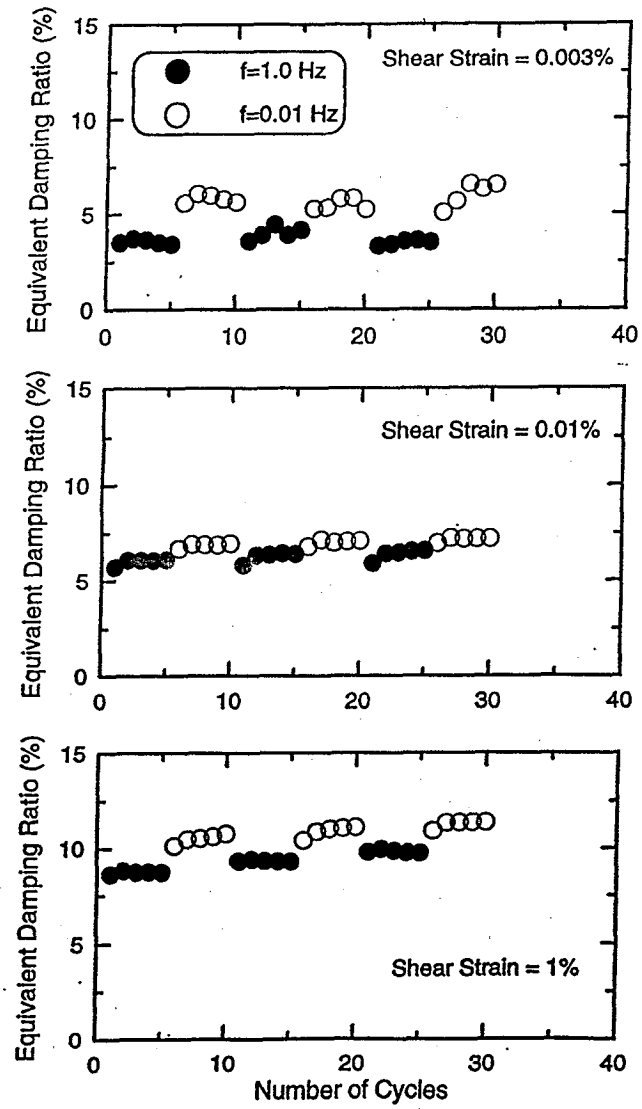

FIG. 7. Effect of Loading Frequency and Number of Cycles on Equivalent Damping Ratio for Test No. 12

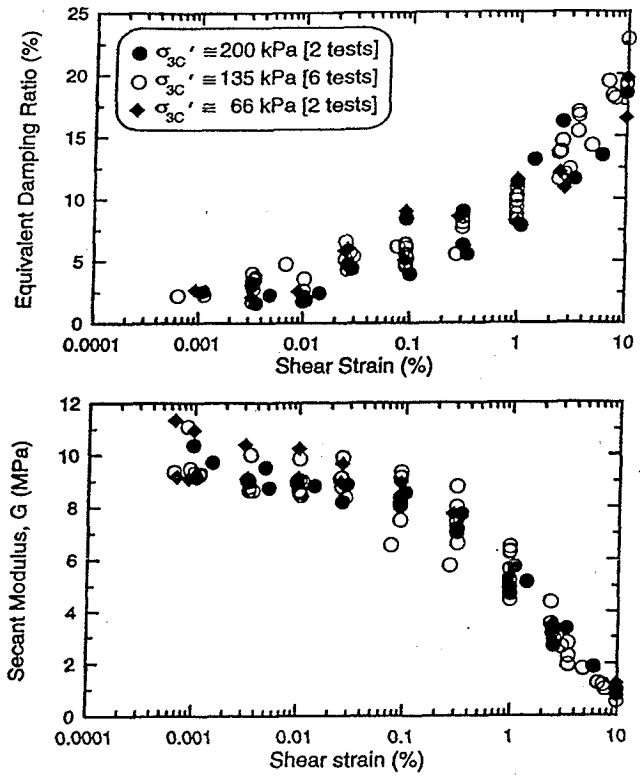

FIG. 8. Summary of Secant Modulus and Equivalent Damping Ratios versus Shear Strain

Results for all specimens are summarized in Fig. 8, showing the secant moduli and equivalent damping ratios versus shear strain for the fifth cycle of loading at a frequency of 1 Hz (0.25 Hz for strains greater than 5%). Nearly linear behavior, in terms of negligible modulus reduction and low damping ratios, was exhibited for shear strains of up to about 0.1%. The specimens that were consolidated to σ'_{3c} of 66 and 200 kPa (closed symbols in Fig. 8) showed behavior very similar to the specimens consolidated to their in situ σ'_{vo} of about 132 kPa (open symbols in Fig. 8). The fact that G_{max} was relatively unaffected as σ'_{3c} ranged from 66 to 200 kPa would be consistent with the peat having a preconsolidation stress that was close to, or greater than, 200 kPa. Preconsolidation stresses of close to 200 kPa are reasonably consistent with the range of consolidation test results by Roger Foott Associates (1991).

The variation in normalized modulus reduction versus shear strain (G/G_{max} versus γ), and equivalent damping ratios versus shear strain, for the fifth cycle of loading on all specimens are shown in Fig. 9. A reasonable representation of the G/G_{max} and equivalent damping ratio data are given on Fig. 9 as upper range, lower range, and median curves. The median G/G_{max} ratio remains greater than 0.90 for shear strains of up to about 0.05% and drops to about 0.50 at shear strains of about 1%. The median damping ratio is less than about 5% for shear strains of up to about 0.05% and increases to about 10% at shear strains of about 1%.

MONOTONIC TESTS

The results of the monotonic, strain-controlled triaxial compression and extension tests are presented in Fig. 10 as plots of normalized deviator stress (q/p'_c) versus axial strain (ε_a) and

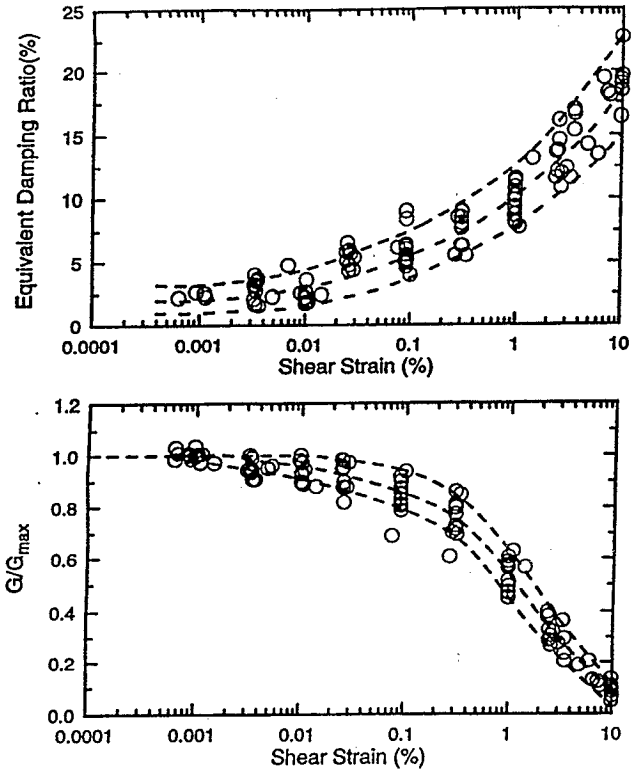

FIG. 9. Upper-Range, Median, and Lower-Range Curves of G/G_{max} and Damping Ratio versus Shear Strain for All Specimens

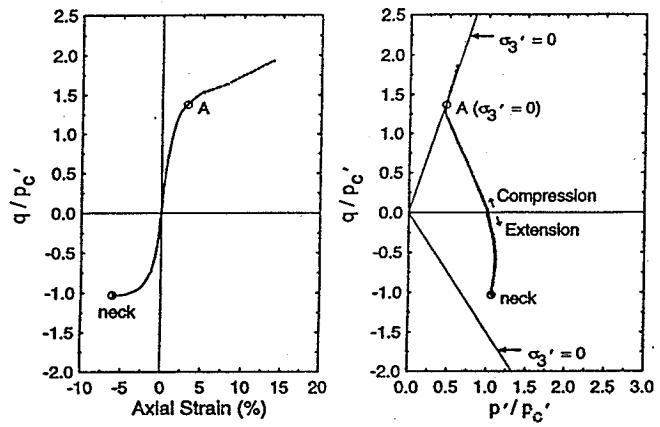

FIG. 10. Monotonic Compression and Extension Test Results

of normalized deviator stress versus normalized mean effective stress (p'/p_c'). These two specimens were isotropically consolidated to a mean effective consolidation stress (p_c') of about 132 kPa, following the same procedures previously described for the cyclic testing program. These tests were run with the drainage lines closed, but the response under compression produces effectively "incrementally drained" behavior past point A in Fig. 10, as will be discussed. The loading rate was about 0.33% axial strain per hour, which was sufficiently slow to allow pore pressure equalization throughout the specimens. (These tests will be called "slow" tests here.)

The compression test showed a progressive increase in excess pore pressure (i.e., decreasing p') and deviator stress (q) as axial strain increased up to point A in Fig. 10. At point A, the pore pressure equaled the radial confining pressure and therefore the radial effective stress (i.e., σ_3') was equal to zero. Beyond point A, the deviator stress continued to increase with no further change in pore pressure; therefore, σ_3' remained equal to zero, and p' was equal to $q/3$. Also, there is a notable decrease in the stiffness of the specimen at point A, as shown by the plot of q versus ε_a in Fig. 10. The specimen's continued resistance to shear while $\sigma_3' = 0$ demonstrates that the reinforcing effects of the organic fibers are extremely important under compressive loading. Note that loading beyond point A resulted in incrementally drained conditions because the confining membrane could easily expand (since $\sigma_3' = 0$) to accommodate movement of pore water toward the lateral boundaries.

The extension test showed a progressive decrease in pore pressure and increase in deviator load (extension) as the extension axial strain was increased. Data are shown only for axial strains of up to −6% because the specimen necked at that point and any additional data became meaningless.

The stress paths (q versus p') for compression (up to point A in Fig. 10) and extension show that the peat specimens exhibit strong cross-anisotropic behavior: Specimens are effectively stiffer in the horizontal direction than in the vertical direction. Recall that triaxial compression or extension loading of a saturated isotropic elastic material would result in a vertical stress path on the q versus p' diagram. For soils without strong cross-anisotropy, the stress path is nearly vertical at small loading levels and then curves as the soil yields. The stress path for the compression test in Fig. 10 is almost linear from the start of compressive loading to point A, and the stress paths for both the compression and extension tests are clearly inclined to the left for small levels of loading. The initial inclination of these stress paths cannot be attributed to plastic deformations because the material is nearly linear elastic at these load levels. These stress paths would be expected for cross-anisotropic elastic materials that are stiffer in the horizontal direction than in the vertical direction (Graham and Houlsby 1983).

"Fast" monotonic loading tests using more conventional rates of loading (e.g., 15% axial strain per hour) on peat specimens resulted in unreliable measurements of pore pressure (Boulanger et al. 1997). The need for "slow" monotonic loading to obtain reliable measurements of pore pressure, and therefore of effective stress, in clay specimens has been emphasized by Zergoun and Vaid (1994). The effect of loading rate on pore pressure measurements appears to be much greater for the Sherman Island peat than for clay. Possible causes of this include peat's highly fibrous fabric, strong cross-anisotropy, high compressibility, scale effects (i.e., specimen size versus characteristic particle or fiber size), boundary effects (nonuniformities of stress or strain within the specimen), and other factors not yet understood.

COMPARISON OF MODULUS REDUCTION AND DAMPING RELATIONSHIPS

In Fig. 11, the median modulus reduction and damping relationships for the peat specimens (Fig. 9) are compared with the curves recommended by Vucetic and Dobry (1991) for normally and overconsolidated clays of varying plasticity. The peat specimens showed a response that is roughly comparable to that of high-plasticity clays with PIs of 100–200. This relatively linear behavior agrees with Stokoe et al.'s (1996) data for peat from a similar range of consolidation stresses. The behavior is much more linear than that observed by Kramer (1996) for unconsolidated peat, but Kramer also observed that the behavior became more linear with increasing consolidation stress; therefore, the difference may be due to consolidation stress.

The median modulus reduction and damping relationships for the peat specimens are compared, in Fig. 12, to curves for Union Bay peat, derived by Seed and Idriss (1970), and curves for solid waste materials, derived primarily from the recorded earthquake motions at the OII landfill by Idriss et al. (1995), GeoSyntec (1996), and Augello et al. (1997). This comparison

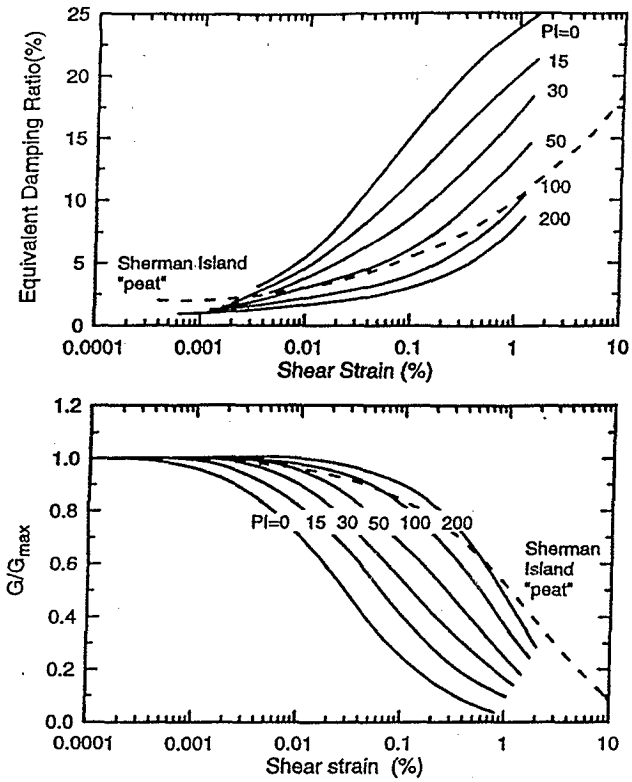

FIG. 11. Median G/G_{max} and Damping Ratio Curves for Sherman Island Peat versus Curves Recommended by Vucetic and Dobry (1991) for Normally Consolidated and Overconsolidated Clays of Varying Plasticity

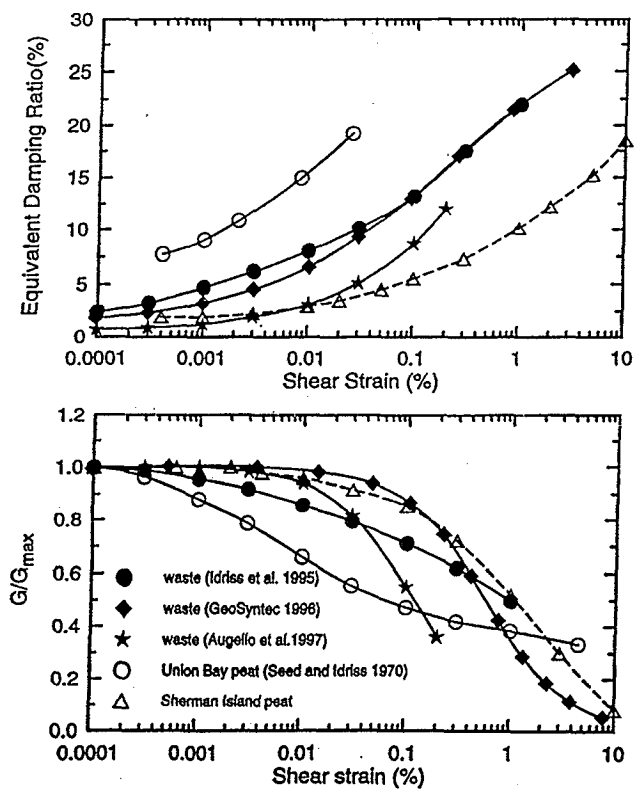

FIG. 12. G/G_{max} and Damping Ratio Curves for Sherman Island Peat versus Curves for Union Bay Peat and Solid Waste Materials

is of interest because it has often been suggested that solid waste materials and peat may have similar modulus reduction and damping relationships. As shown in Fig. 12, the curves for Sherman Island peat generally show the least modulus reduction, with the closest similarity to the curves by Idriss et al. (1995) and Geosyntec (1996). The damping ratio curves for Sherman Island peat are generally lower (i.e., more linear) than any of the other curves.

The G_{max} values obtained from the bender element tests on the peat specimens were about 20% smaller than those obtained from the direct stress-strain measurements, as shown in Fig. 5 for test no. 1. This difference in G_{max} could be partly due to the second-arrival method slightly underestimating V_s, the effects of boundary conditins on triaxial tests results, and the effects of structural anisotropy (the peat may be softer under the horizontal shearing produced by the bender element tests than under the axial loading condition used to obtain stress-strain measurements). Strong cross-anisotropic behavior of the peat was clearly indicated by the effective stress paths during monotonic compression and extension loading, and this behavior is consistent with the visible layering of fibers within the specimens. Additional research is needed to investigate how structural anisotropy and other factors—such as loading path or specimen size—may affect the modulus reduction and damping relationships for peat.

SUMMARY

This report summarizes the results of a laboratory study of the dynamic properties of a layer of peaty organic soil underlying the south levee on Sherman Island near the western side of the Sacramento–San Joaquin Delta. Shelby tube samples were obtained from depths of about 13 m where the vertical consolidation stresses (σ'_{vc}) were about 132 kPa. The samples tested were very fibrous and had ash contents of 35–56%. Staged cyclic loading was used to measure the stress-strain behavior of several specimens under cyclic shear strains ranging from about 0.0005% to 10%. The experimental procedures and results were presented in detail because only limited experimental data are currently available for peat and peaty organic soils.

The modulus reduction and damping relationships for the Sherman Island peat were roughly comparable to those recommended for high-plasticity clays (PI of 100–200) by Vucetic and Dobry (1991). Secant shear moduli and damping were found to depend somewhat on loading frequency and were relatively unaffected by cyclic degradation. The relatively linear behavior of Sherman Island peat agrees with Stokoe et al.'s (1996) data for two peat samples with similar ash contents and consolidation stresses.

Modulus reduction and damping relationships for peat may depend on numerous factors that have not yet been explored, including loading path and specimen size. Additional laboratory testing is needed on samples from other sites, covering a range of material characteristics (e.g., ash content, fabric) and consolidation stress conditions. Extrapolation of the results presented in this paper to other conditions must consider these uncertainties.

ACKNOWLEDGMENTS

Support for this research was provided by the U.S. Geological Survey (USGS), Department of Interior, under USGS award number 1434-95-G-2531, and the Department of Water Resources (CDWR), State of California. The views and conclusions contained in this document are those of the authors and should not be interpreted as necessarily representing the official policies, either expressed or implied, of the U.S. government or the State of California. The National Science Foundation funded acquisition of the triaxial equipment under NSF award number BCS-9310669 and of the bender element equipment under NSF award number CMS-9502530. Brent Lampkin assisted with the drilling and sampling work. William Gookin assisted with the laboratory testing. All the support and assistance is greatly appreciated.

APPENDIX. REFERENCES

Arulnathan, R., Boulanger, R. W., and Riemer, M. F. (1997). "Analysis of bender element tests." *Geotech. Testing J.*, ASTM.

Augello, A., Bray, J. D., Abrahamson, N. A., and Seed, R. B. (1998). "Dynamic properties of solid-waste based on back-analysis of the OII landfill." *J. Geotech. and Geoenviron. Engrg.*, ASCE, 124(2).

Boulanger, R. W., Arulnathan, R., Harder, L. F. Jr., and Torres, R. A. (1997). "Dynamic properties of Sherman Island peat," *Rep. No. UCD/CGM-97/01*, Ctr. for Geotech. Modeling, Univ. of California, Davis, Calif.

GeoSyntec. (1996). "Summary report of findings, seismicity, settlement, and slope stability work plan, Operating Industries, Inc., Landfill, Monterey Park, California." *Rep. No. SWP-9*, GeoSyntec Consultants, Huntington Beach, Calif.

Gookin, W. B., Riemer, M. F., Boulanger, R. W., and Bray, J. D. (1996). "Development of cyclic triaxial apparatus with broad frequency and strain ranges." *Transp. Res. Rec. 1548*, 1–8.

Graham, J., and Houlsby, G. T. (1983). "Anisotropic elasticity of a natural clay." *Geotechnique*, 33(2), 165–180.

Idriss, I. M., Dobry, R., and Singh, R. D. (1978). "Nonlinear behavior of soft clays during cyclic loading." *J. Geotech. Engrg. Div.*, ASCE, 104(12), 1427–1447.

Idriss, I. M., Fiegel, G., Hudson, M. B., Mundy, P. K., and Herzog, R. (1995). "Seismic response of the Operating Industries Landfill." *Proc., Earthquake Des. and Performance of Solid Waste Landfills, Geotech. Special Pub. No. 54*, ASCE, New York, N.Y., 83–118.

Kramer, S. L. (1993). "Seismic response: Foundations in soft soils." *Final Res. Rep. WA-RD 264.1*, Washington State Transp. Ctr., Univ. of Washington, Seattle, Wash.

Kramer, S. L. (1996). "Dynamic response of peats." *Final Res. Rep. WA-RD 412.1*, Washington State Transp. Ctr., Univ. of Washington, Seattle, Wash.

Roger Foott Associates, Inc. (1991). "Investigation and treatment of threatened levees on Sherman Island." *Job No. 085-002*, San Francisco, Calif.

Seed, H. B., and Idriss, I. M. (1970). "Analyses of ground motions at Union Bay, Seattle, during earthquakes and distant nuclear blasts." *Bull. Seismological Soc. of America*, 60(1), 125–136.

Seismic stability evaluation of the Sacramento–San Joaquin Delta levees. Phase I report: Preliminary evaluations and review of previous studies. (1992). Div. of Des. and Constr., Dept. of Water Resour., State of California.

Stokoe, K. H. II, Bay, J. A., Rosenblad, B. L., Hwang, S.-K., and Twede, M. R. (1996). "In situ seismic and dynamic laboratory measurements of geotechnical materials at Queensboro Bridge and Roosevelt Island." *Geotech. Engrg. Rep. GR94-5*, Civ. Engrg. Dept., Univ. of Texas at Austin.

Tatsuoka, F., Teachavorasinskun, S., Dong, J., Kohata, Y., and Sata, T. (1994). "Importance of measuring local strains in cyclic triaxial tests on granular materials." *Dynamic geotechnical testing II: ASTM STP 1213*, R. J. Ebelhar, V. P. Drnevich, and B. L. Kutter, eds., American Society for Testing and Materials, Philadelphia, Pa., 288–302.

Tatsuoka, F., Shibuya, S., and Teachavorasinskun, S. (1991). "Discussion of 'Shear modulus and cyclic undrained behavior of sands,' by Alarcon-Guzman, A., Chameau, J. L., Leonards, G. A., and Frost, J. D.," *Soils and Foundations*, 31(2), 202–209.

Vucetic, M., and Dobry, R. (1991). "Effect of soil plasticity on cyclic response." *J. Geotech. Engrg.*, ASCE, 117(1), 89–107.

Zergoun, M., and Vaid, Y. P. (1994). "Effective stress response of clay to undrained cyclic loading." *Can. Geotech. J.*, 31, 714–727.